Spontaneous and piezoelectric polarization effects in III–V nitride heterostructures

E. T. Yu,[a] X. Z. Dang, P. M. Asbeck, and S. S. Lau
Department of Electrical and Computer Engineering, University of California at San Diego, La Jolla, California 92093-0407

G. J. Sullivan
Rockwell Science Center, Thousand Oaks, California 91358

(Received 19 January 1999; accepted 3 May 1999)

The role of spontaneous and piezoelectric polarization in III–V nitride heterostructures is investigated. Polarization effects and crystal polarity are reviewed in the context of nitride heterostructure materials and device design, and a detailed analysis of their influence in nitride heterostructure field-effect transistors is presented. The combined effects of spontaneous and piezoelectric polarization are found to account well for carrier concentrations observed in AlGaN/GaN transistor structures with low to moderate Al concentrations, while the data for higher Al concentrations are consistent with defect formation in the AlGaN barrier. Theoretical analysis suggests that incorporation of In into the barrier and/or channel layers can substantially increase polarization charge at the heterojunction interface. The use of polarization effects to engineer Schottky barrier structures with large enhancements in barrier height is also discussed, and electrical characteristics of transistors with conventional and polarization-enhanced Schottky barrier gates are presented. The polarization-enhanced barrier is found to yield a marked reduction in gate leakage current, but to have little effect on transistor breakdown voltage. © *1999 American Vacuum Society*. [S0734-211X(99)05804-7]

I. INTRODUCTION

III–V nitride heterostructures are of outstanding current interest for a wide range of device applications, including blue and ultraviolet light-emitting diodes and lasers,[1] high-temperature/high-power electronics,[2–6] visible-blind ultraviolet photodetectors,[7,8] and field-emitter structures.[9,10] In addition, these materials, by virtue of their wurtzite crystal structure and high degree of ionicity, exhibit a variety of material properties that either are not found or are of considerably reduced importance in conventional zincblende III–V semiconductors. Of particular interest are piezoelectric and spontaneous polarization effects, which recent experimental and theoretical investigations have revealed to be of great importance in the design and analysis of nitride heterostructure devices,[11–14] and which can be exploited to advantage in nitride materials and device engineering.

In this article, we review the basic phenomena of spontaneous and piezoelectric polarization in nitride semiconductors and discuss their role in nitride heterostructure device physics, with particular emphasis on the design and analysis of nitride-based heterostructure field-effect transistors (HFETs). Section II provides an overview of piezoelectric and spontaneous polarization effects in nitride heterostructures, the influence of crystal polarity, and the role of polarization effects in the analysis and design of various nitride heterostructure devices. Section III focuses specifically on the role of spontaneous and piezoelectric polarization in the analysis and design of nitride HFETs; the use of polarization effects to engineer Schottky barrier structures in nitride HFETs is addressed in Sec. IV. Section V concludes the article.

II. OVERVIEW OF POLARIZATION EFFECTS

The wurtzite crystal structure of nitride semiconductors combined with epitaxial growth that is performed typically in the (0001) orientation leads to the existence of a piezoelectric polarization field and associated electrostatic charge densities in strained material that have been shown to influence carrier distributions, electric fields, and consequently a wide range of optical and electronic properties of nitride materials and devices. In addition, recent theoretical results have indicated that nitride semiconductors also possess a large spontaneous polarization,[15] associated with which will be electrostatic charge densities analogous to those produced by piezoelectric polarization fields. In bulk material it is assumed that rearrangement of surface charges nullifies spatially uniform piezoelectric and spontaneous polarization fields. In heterostructures or inhomogeneous alloy layers, however, variations in composition are expected to create nonvanishing spontaneous and piezoelectric polarization fields and associated charge densities that can dramatically influence material properties and device behavior.

The piezoelectric polarization field $\mathbf{P}_{\mathrm{pz}}$ is determined by the piezoelectric coefficients e_{ij} and the strain tensor ϵ_j, and is given by

$$\mathbf{P}_{\mathrm{pz}}=e_{ij}\epsilon_j=d_{ij}c_{jk}\epsilon_k, \quad j,k=xx,yy,zz,yz,zx,xy, \tag{1}$$

where d_{ij} are the piezoelectric coefficients relating the polarization to the stress tensor $\sigma_j=c_{jk}\epsilon_k$, and c_{jk} is the elastic tensor. Contracted matrix notation is used, and summation

[a]Electronic mail: ety@ece.ucsd.edu

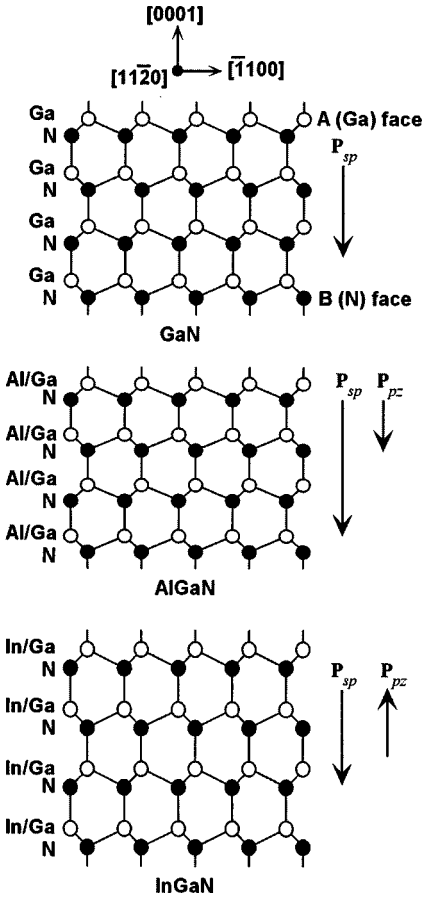

FIG. 1. Crystal structure, spontaneous polarization fields ($\mathbf{P}_{sp}$) and piezoelectric polarization fields ($\mathbf{P}_{pz}$) for GaN (top), and for $Al_xGa_{1-x}N$ and $In_yGa_{1-y}N$ coherently strained to GaN (0001).

over repeated indices is assumed. The total polarization field $\mathbf{P}$ is then the sum of $\mathbf{P}_{pz}$ and the spontaneous polarization $\mathbf{P}_{sp}$, and is related to the polarization charge density ρ_{pol} according to

$$\nabla \mathbf{P} = \nabla \cdot (\mathbf{P}_{sp} + \mathbf{P}_{pz}) = -\rho_{pol}. \tag{2}$$

From Eq. (2) it is evident that at an abrupt heterojunction interface, a polarization sheet charge density will be present arising from the difference in spontaneous polarization between the two heterojunction constituents and from the abrupt change in strain ϵ_j that gives rise to a discontinuity in $\mathbf{P}_{pz}$. In compositionally graded alloy layers, the spatially varying polarization field will produce either positive or negative volume charge densities that will in many respects act as donors or acceptors, respectively. Finally, it should be noted that very gradual changes in $\mathbf{P}$, as would arise from uniform or nearly uniform stress in an epitaxial layer structure, will produce only very small polarization charge densities.

Closely related to the investigation of polarization and its influence on nitride heterostructure device physics is the issue of crystal polarity. Figure 1 shows a schematic diagram of the GaN wurtzite crystal structure. The lack of inversion symmetry in the (0001) plane gives rise to two possible polarities for (0001) epitaxial growth. The upper (0001) surface in the figure is referred to as the A (or Ga) face, and the lower $(000\bar{1})$ surface as the B (or N) face. It has been found empirically that the orientation of high-quality nitride films grown by metalorganic chemical vapor deposition (MOCVD) is typically (0001), whereas molecular-beam epitaxy (MBE) can yield high-quality films with either the (0001) or the $(000\bar{1})$ orientation. (0001) and $(000\bar{1})$ films can be distinguished from each other by a variety of techniques including wet chemical etching, characterization of physical morphology, and convergent beam electron diffraction.[16]

Polarity in epitaxially grown nitride films is significant in the context of polarization because the spontaneous and piezoelectric polarization fields have a well-defined orientation with respect to the A and B crystal faces. Theoretical calculations[15] indicate that for GaN, AlN, and InN the spontaneous polarization field is in the $[000\bar{1}]$ direction, i.e., pointing from the A face to the B face as indicated in Fig. 1. Experimental[12,13] and theoretical[15] results have indicated that the signs of the relevant piezoelectric coefficients in the nitrides are such that for (0001) films grown under tensile or compressive strain, $\mathbf{P}_{pz}$ is in the $[000\bar{1}]$ or [0001] direction, respectively. The orientation of the piezoelectric polarization field with respect to the crystallographic axes in the nitride semiconductors is opposite that found in other III–V semiconductors and is the same as that found in II–VI semiconductors, a consequence of the greater ionicities of III–V nitrides compared to those of other III–V semiconductors.[13,15,17]

For strained III–V nitride epitaxial layers grown in the (0001) orientation, a piezoelectric polarization will be present aligned along the [0001] direction and given by

$$P_{pz,z} = 2\left(e_{31} - \frac{c_{13}}{c_{33}} e_{33}\right)\epsilon_1. \tag{3}$$

The values of the spontaneous polarization and of the relevant piezoelectric and elastic constants in III–V nitrides have in many cases not been definitively established. Table I shows values for several relevant physical quantities for GaN, AlN, and InN.[18–32] In this work, we have used theoretical values[15] for spontaneous polarization and for the piezoelectric coefficients e_{31} and e_{33}. For spontaneous polarization, only a single set of theoretical values, and no experimental values, are available. For the piezoelectric coefficients, only theoretical values are available for InN; for AlN, experimental and theoretical values appear to be in good agreement. In the case of GaN, there is a significant discrepancy between the experimental and theoretical values, particularly for e_{31}; for consistency, and given the large uncertainty likely to exist for both the experimental and theoretical values, we have used the theoretical values for e_{31} and e_{33}. For the elastic constants c_{13} and c_{33}, we have used the averages of the values listed in Table I. Values for ternary and quaternary alloys are then obtained by simple linear interpolation.

Recent work has demonstrated that polarization effects can exert a pronounced influence on heterostructure material

TABLE I. Selected physical constants for GaN, AlN, and InN.

	GaN	AlN	InN	Reference
a (Å)	3.189	3.112	3.548	18
c (Å)	5.185	4.982	5.760	18
e_{31} (C/m^2)	−0.32	⋯	⋯	20
e_{31} (C/m^2)	−0.22	⋯	⋯	21
e_{31} (C/m^2)	−0.36	⋯	⋯	19, 22
e_{31} (C/m^2)	⋯	−0.58	⋯	23
e_{31} (C/m^2)	−0.49	−0.60	−0.57	15
e_{33} (C/m^2)	0.65	⋯	⋯	20
e_{33} (C/m^2)	0.44	⋯	⋯	21
e_{33} (C/m^2)	1	⋯	⋯	19, 22
e_{33} (C/^{2})	⋯	1.55	⋯	23
e_{33} (C/m^2)	0.73	1.46	0.97	15
c_{13} (GPa)	158	⋯	⋯	24
c_{13} (GPa)	70	⋯	⋯	25
c_{13} (GPa)	106	⋯	⋯	26
c_{13} (GPa)	114	⋯	⋯	27
c_{13} (GPa)	110	100	⋯	28
c_{13} (GPa)		120	⋯	29
c_{13} (GPa)		99	⋯	30
c_{13} (GPa)	100	127	94	31
c_{13} (GPa)	103	108	92	32
c_{33} (GPa)	267	⋯	⋯	24
c_{33} (GPa)	379	⋯	⋯	25
c_{33} (GPa)	398	⋯	⋯	26
c_{33} (GPa)	209	⋯	⋯	27
c_{33} (GPa)	390	390	⋯	28
c_{33} (GPa)	⋯	395	⋯	29
c_{33} (GPa)	⋯	389	⋯	30
c_{33} (GPa)	392	382	200	31
c_{33} (GPa)	405	373	224	32
$P_{sp,z}$ (C/m^2)	−0.029	−0.081	−0.032	15

properties and device physics, and furthermore that these effects can be used to achieve substantial improvements in various aspects of device performance. In $In_yGa_{1-y}N$/GaN quantum well structures, polarization fields in the $In_yGa_{1-y}N$ quantum wells lead to substantial redshifts in luminescence energy that are screened at high carrier concentrations.[33–37] Recently, it has also been shown that local strain fields associated with threading dislocations can create substantial electrostatic sheet charge densities, and consequently electric fields, at a free surface or a heterojunction interface in the vicinity of the dislocation.[38] In $Al_xGa_{1-x}N$/GaN HFETs, positive polarization charge at the $Al_xGa_{1-x}N$/GaN interface contributes to the formation of a two-dimensional electron gas (2DEG) with extremely high carrier concentrations.[12,13] Furthermore, polarization charges can be used in a nitride HFET to achieve a dramatic increase in barrier height, and consequently a reduction in gate leakage current, without increasing the total barrier thickness or the Al concentration in the $Al_xGa_{1-x}N$ layer.[39] Finally, polarization charges in compressively strained $In_yGa_{1-y}N$ deposited on GaN can be used to lower the surface barrier, and consequently decrease turn-on voltage, for GaN field emitters.[40]

III. POLARIZATION EFFECTS IN HFETs

It has emerged from studies of $Al_xGa_{1-x}N$/GaN HFETs that polarization charges at the $Al_xGa_{1-x}N$/GaN interface are a dominant factor in the formation of a 2DEG with extremely high carrier concentration at the heterojunction interface.[12,13] For an $Al_xGa_{1-x}N$/GaN HFET epitaxial layer structure, the $Al_xGa_{1-x}N$ will be under tensile strain and, for growth on the (0001) surface (i.e., A or Ga face), a positive polarization charge density will be present at the $Al_xGa_{1-x}N$/GaN heterojunction interface. For growth on the (0001) surface, the polarization sheet charge density $\sigma_{\rm pol}$ at the heterojunction interface and the electron sheet concentration n_s in the 2DEG will be given approximately by

$$n_s=\sigma_{\rm pol}/e-(\epsilon_{\rm AlGaN}/de^2)(e\phi_b+E_F-\Delta E_c)+\tfrac{1}{2}N_d\,d, \quad (4)$$

$$\sigma_{\rm pol}/e=-2[e_{31}-(c_{13}/c_{33})e_{33}](a_{\rm GaN}/a_{\rm AlN}-1)x + P^{\rm GaN}_{{\rm sp},z}-P^{AlGaN}_{{\rm sp},z}, \quad (5)$$

where e_{31}, e_{33}, c_{13}, and c_{33} are the relevant piezoelectric and elastic constants for $Al_xGa_{1-x}N$, $a_{\rm GaN}$ and $a_{\rm AlN}$ are the lattice constants of GaN and AlN, respectively, $P^{\rm GaN}_{{\rm sp},z}$ and $P^{\rm AlGaN}_{{\rm sp},z}$ are the spontaneous polarizations of GaN and $Al_xGa_{1-x}N$, $\epsilon_{\rm AlGaN}$ is the dielectric constant of $Al_xGa_{1-x}N$, ϕ_b is the $Al_xGa_{1-x}N$ Schottky barrier height, E_F and ΔE_c are the Fermi energy and conduction-band offset, respectively, at the heterojunction interface, and d and N_d are the thickness and donor concentration, respectively, in the $Al_xGa_{1-x}N$ barrier layer.

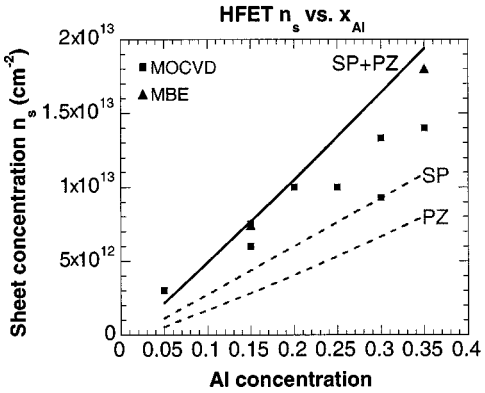

FIG. 2. Measured (symbols) and calculated (lines) sheet carrier concentrations in $Al_xGa_{1-x}N$/GaN HFET structures grown by both MBE and MOCVD as a function of Al concentration. Calculated values show the separate and combined contributions of piezoelectric and spontaneous polarization.

Figure 2 shows n_s (obtained from Hall measurements) as a function of Al concentration for a series of 300 Å $Al_xGa_{1-x}N$/GaN HFET structures grown by both MBE and MOCVD. Also shown are values of n_s calculated from Eqs. (4) and (5) using values for e_{31}, e_{33}, c_{13}, and c_{33} determined in the manner described above, and assuming $N_d=1\times10^{18}\,{\rm cm}^{-3}$. For Al concentrations below ~20%, the agreement between the calculated and measured values is very good, provided that the contributions of both spontaneous and piezoelectric polarization charge are included. For higher Al concentrations, the measured values for n_s are significantly below the calculated values. Estimates of strain relaxation in $Al_{0.25}Ga_{0.75}N$/GaN HFETs[41] have indicated that

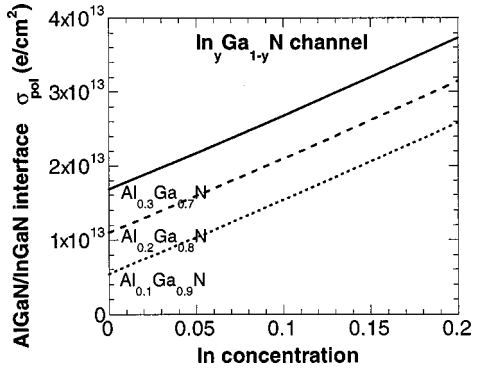

FIG. 3. Polarization sheet charge concentration at the 2DEG interface of an HFET structure containing an $Al_xGa_{1-x}N$ barrier and $In_yGa_{1-y}N$ channel, shown for Al concentrations of 10%, 20%, and 30% as a function of In concentration.

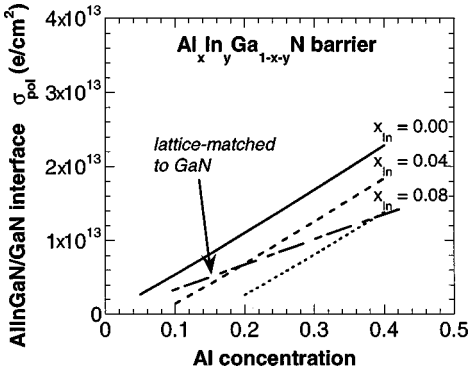

FIG. 4. Polarization sheet charge concentration at the 2DEG interface of an HFET structure containing an $Al_xIn_yGa_{1-x-y}N$ barrier layer, shown for In concentrations of 0%, 4%, and 8% as a function of Al concentration. For barriers lattice matched to GaN, the polarization charge density increases with In concentration.

strain relaxation initiates for $Al_{0.25}Ga_{0.75}N$ layer thicknesses between 20 and 40 nm, suggesting that the discrepancy between our calculated and measured values at Al concentrations above ~20% may be due partly to strain relaxation and, consequently, a reduction in piezoelectric polarization charge, or possibly to formation of compensating defects in the $Al_xGa_{1-x}N$ layer.

The analysis of sheet carrier concentration as a function of composition can be extended to include In-containing alloys. Because of the relatively large lattice mismatch between InN and GaN compared to that between AlN and GaN (11.3% and 2.4%, respectively), low In concentrations in an $In_yGa_{1-y}N$ alloy will lead to relatively high piezoelectric charge densities at an $In_yGa_{1-y}N$/GaN heterojunction interface. Because $In_yGa_{1-y}N$ grown on GaN will be under compressive strain, a negative piezoelectric sheet charge density will be present at the bottom of the $In_yGa_{1-y}N$ layer and a positive sheet charge density at the top, for growth on the (0001) surface. Incorporation into an HFET structure of an $In_yGa_{1-y}N$ channel layer with an $Al_xGa_{1-x}N$ barrier should therefore lead to a substantial increase in polarization charge density at the 2DEG interface, as shown in Fig. 3. The major additional contribution to polarization charge is expected to be piezoelectric, since the calculated values of spontaneous polarization for GaN and InN differ by only a small amount.

An additional possibility is incorporation of an $Al_xIn_yGa_{1-x-y}N$ barrier into an HFET structure. Incorporation of In into the barrier layer will allow higher Al concentrations to be attained without strain relaxation. Because the discontinuity in spontaneous polarization is expected to provide a larger contribution to polarization charge at the heterojunction interface than piezoelectric polarization for a given change in Al concentration, an $Al_xIn_yGa_{1-x-y}N$ barrier structure may be expected to provide a substantial polarization sheet charge (due to spontaneous polarization) even at compositions lattice matched to GaN as shown in Fig. 4. Furthermore, for a given degree of tensile strain the polarization charge at the $Al_xIn_yGa_{1-x-y}N$/GaN interface is expected to increase with In concentration, and consequently the maximum polarization charge density that can be achieved without strain relaxation in the barrier layer will also increase with In concentration.

IV. SCHOTTKY BARRIER ENHANCEMENT IN NITRIDE HFETs

As an example of the use of polarization effects to improve various aspects of device performance, we describe recent studies in which polarization effects were used to achieve large increases in Schottky barrier height in an $Al_xGa_{1-x}N$/GaN HFET structure,[39] and in which the influence of this increase on transistor characteristics was investigated. Figure 5(a) shows a schematic energy band diagram for an HFET epitaxial layer structure in which the barrier incorporates a thin GaN layer grown on top of the conventional $Al_xGa_{1-x}N$ barrier. Figure 5(b) shows the correspond-

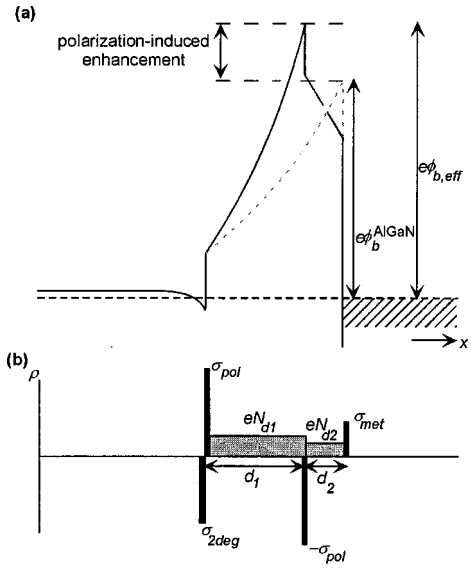

FIG. 5. (a) Schematic energy band diagram and (b) charge distribution for an HFET structure in which the barrier consists of GaN grown atop $Al_xGa_{1-x}N$. The negative polarization sheet charge at the upper $Al_xGa_{1-x}N$/GaN interface leads to a large enhancement in effective barrier height.

ing charge distribution in this structure, assuming growth on the (0001) surface. As shown in Fig. 5, incorporation of a GaN layer above the $Al_xGa_{1-x}N$ barrier layer allows the negative polarization charge at the top of the $Al_xGa_{1-x}N$ layer to be positioned within the Schottky barrier structure, thereby increasing the effective barrier height. This approach is analogous to the use of a thin p^+ layer near the metal–semiconductor interface of an *n*-type Schottky diode to increase the effective barrier height electrostatically. In the structure shown in Fig. 5(a), however, control over layer thickness and composition in epitaxial growth allows the magnitude and position of the polarization charge to be controlled very precisely.

A straightforward electrostatic analysis shows that the 2DEG sheet concentration n_s and the effective barrier height $\phi_{b,\mathrm{eff}}$ are given by

$$n_s=\frac{\sigma_{\mathrm{pol}}-(\epsilon_{\mathrm{AlGaN}}/d_1)(\phi_b^{\mathrm{GaN}}+E_F/e-V)+eN_{d1}d_1/2+(\epsilon_{\mathrm{AlGaN}}/\epsilon_{\mathrm{GaN}})(eN_{d1}d_2+eN_{d2}d_2^2/2d_1)}{e[1+(\epsilon_{\mathrm{AlGaN}}/\epsilon_{\mathrm{GaN}})(d_2/d_1)]}, \tag{6}$$

$$\phi_{b,\mathrm{eff}}=\Delta E_c/e+\phi_b^{\mathrm{GaN}}+\frac{ed_2}{\epsilon_{\mathrm{GaN}}}(n_s-N_{d1}d_1-N_{d2}d_2), \tag{7}$$

where σ_{pol} is the $GaN/Al_xGa_{1-x}N$ interface polarization sheet charge density (including both spontaneous and piezoelectric polarization), d_1 and d_2 are the $Al_xGa_{1-x}N$ and GaN layer thicknesses, N_{d1} and N_{d2} are the $Al_xGa_{1-x}N$ and GaN layer donor concentrations, $\epsilon_{\mathrm{AlGaN}}$ and ϵ_{GaN} are the dielectric constants, ϕ_b^{GaN} is the GaN Schottky barrier height, ΔE_c is the conduction-band offset, and E_F is the Fermi level at the 2DEG interface. In deriving Eqs. (6) and (7) we have assumed that $\phi_b^{\mathrm{AlGaN}}=\phi_b^{\mathrm{GaN}}+\Delta E_c$, as suggested by direct measurements of n-$Al_xGa_{1-x}N$ Schottky barrier heights.[42]

Figures 6(a) and 6(b) show, respectively, the effective barrier heights $\phi_{b,\mathrm{eff}}$ and sheet carrier concentrations n_s calculated as functions of GaN layer thickness d_2 for a total barrier thickness d_1+d_2 of 300 Å, assuming $N_{d1}=1\times10^{18}\,\mathrm{cm}^{-3}$, $N_{d2}=5\times10^{17}\,\mathrm{cm}^{-3}$, and $\phi_b^{\mathrm{GaN}}=1.0\,\mathrm{V}$, and showing both the separate and combined effects of the spontaneous and piezoelectric contributions to polarization charge. The total barrier thickness was kept at 300 Å because in an HFET device it is desirable to maintain a small barrier thickness to ensure a high gate capacitance and, consequently, high channel conductance and transconductance. Figure 6 shows that extremely large increases in barrier height may be expected, particularly for higher Al concentrations, when a thin GaN layer is incorporated at the top of the barrier. However, the sheet concentration decreases with increasing GaN layer thickness, necessitating a tradeoff between n_s and $\phi_{b,\mathrm{eff}}$ in selecting an optimum GaN layer thickness.

Measurements of n_s by capacitance–voltage profiling and of $\phi_{b,\mathrm{eff}}$ by photoresponse have shown that for an HFET structure consisting of 225 Å $Al_{0.25}Ga_{0.75}N$/75 Å GaN grown by MOCVD on nominally undoped GaN on a sapphire substrate, an effective barrier height of $1.89\pm0.05\,\mathrm{V}$ and a sheet carrier concentration of $4.5\times10^{12}\,\mathrm{cm}^{-2}$ are obtained. In comparison, a barrier height of $1.52\pm0.05\,\mathrm{V}$ and a sheet carrier concentration of $5.0\times10^{12}\,\mathrm{cm}^{-2}$ are obtained for a control HFET structure with a 300 Å $Al_{0.25}Ga_{0.75}N$ barrier.[39] The extremely large increase in effective barrier height of 0.37 V and the sheet carrier concentrations observed in these structures are consistent with those expected when either spontaneous or piezoelectric polarization effects are included, but are smaller than those expected from the combined effects of spontaneous and piezoelectric polarization. Studies of similarly grown HFET structures with barriers

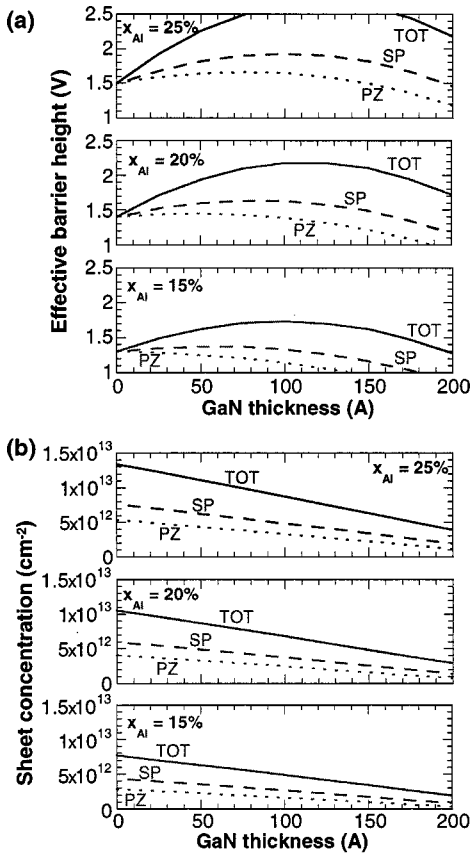

FIG. 6. Calculated values for (a) effective barrier height and (b) electron sheet concentration in a polarization-enhanced HFET Schottky barrier structure, shown as functions of GaN layer thickness for a total barrier thickness of 300 Å, for Al concentrations of 15%, 20%, and 25%. The separate and combined influences of spontaneous (SP) and piezoelectric (PZ) polarization are shown.

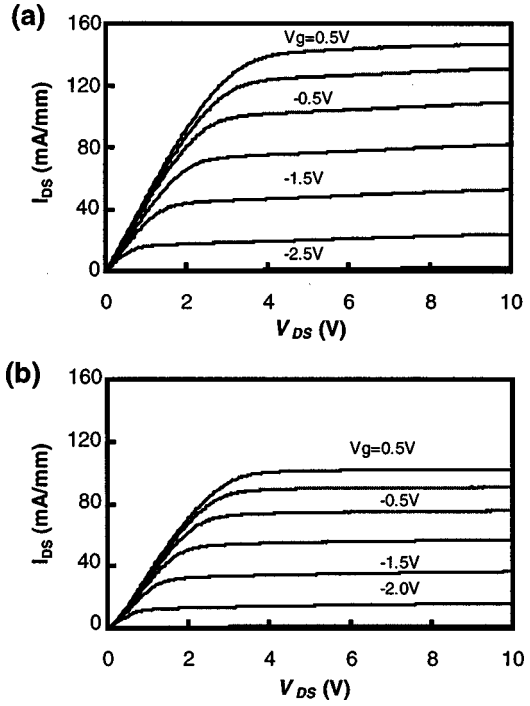

FIG. 7. Current–voltage characteristics for (a) an HFET with a conventional 300 Å $Al_{0.25}Ga_{0.75}N$ barrier and (b) an HFET with a polarization-enhanced 225 Å $Al_{0.25}Ga_{0.75}N$/75 Å GaN barrier.

consisting of 225 Å $Al_{0.30}Ga_{0.70}N$/75 Å GaN and 300 Å $Al_{0.30}Ga_{0.70}N$ have shown that the barrier height changes from 1.56 ± 0.05 V to 1.83 ± 0.05 V with incorporation of the top GaN layer, an increase of 0.27 V. These observations suggest that at these Al concentrations, partial strain relaxation in the $Al_xGa_{1-x}N$ layers may occur, reducing the contribution of piezoelectric polarization to the charge distribution in the epitaxial layer structure. An additional possibility is formation of compensating defects in the $Al_xGa_{1-x}N$ layer at high Al concentrations.

To determine the influence of the observed barrier-height enhancement on HFET device characteristics, transistor structures were fabricated from the epitaxial layer structures described above with barriers consisting of 300 Å $Al_{0.25}Ga_{0.75}N$ (conventional barrier) and 225 Å $Al_{0.25}Ga_{0.75}N$/75 Å GaN (enhanced barrier). Transistors were fabricated with gate lengths of 1 μm and gate widths of 25 and 50 μm, and source-gate and gate-drain spacings of 1 μm each. Ti/Al metallization annealed at 950 °C for 30 s was used for ohmic contacts, and Ni/Au for the Schottky gate contacts.

Figure 7 shows transistor characteristics for the conventional- and enhanced-barrier HFET structures. The enhanced-barrier HFET is characterized by slightly lower drain current and transconductance than the conventional-barrier HFET, features which we attribute primarily to the slightly lower sheet concentration and Hall mobility observed in the enhanced-barrier epitaxial layer structure (4.5×10^{12} cm^{-2} and 620 cm^2/V s at 300 K, in comparison to 5.0×10^{12} cm^{-2} and 800 cm^2/V s for the conventional-barrier

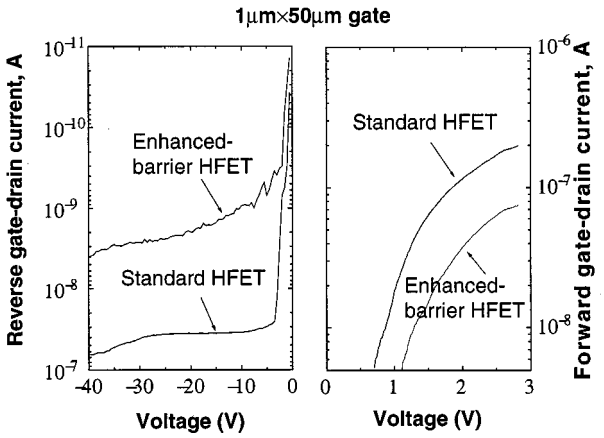

FIG. 8. Gate-drain diode characteristics for the conventional- and enhanced-barrier HFET structures.

structure). Figure 8 shows the gate-drain diode characteristics for these structures. As expected for the enhanced-barrier structure, there is a strong suppression in reverse-bias leakage current—a factor of approximately ten to several hundred—and an increase in forward-bias turn-on voltage of approximately 0.3 V.

A further benefit that might be expected from an increased barrier height is that, if transistor breakdown were to occur primarily via tunneling current through the gate, the enhanced-barrier structure should exhibit a substantially increased breakdown voltage. Detailed investigations of this possibility have been performed using the conventional- and enhanced-barrier HFET device structures. Figure 9 shows the drain and gate currents as functions of the drain-source voltage V_{ds} for the conventional- and enhanced-barrier HFET structures. Defining breakdown to occur at a current of 1 mA/mm, essentially identical breakdown voltages of 98 and 100 V are measured for the enhanced- and conventional-barrier devices. Subsequent analysis of breakdown voltage as a function of temperature has shown that the breakdown voltage increases with increasing temperature, indicating that the primary breakdown mechanism is impact ionization rather than gate tunneling, and explaining the similarity in breakdown voltages measured for the different device structures.[43]

V. CONCLUSIONS

We have investigated the role of spontaneous and piezoelectric polarization in nitride heterostructures, with particular emphasis on the design, characterization, and analysis of nitride HFETs. A detailed understanding of polarization effects and of the closely related issue of crystal polarity is essential in nitride heterostructure materials and device engineering. For $Al_xGa_{1-x}N$/GaN HFETs we have found that, at low to moderate Al concentrations, the 2DEG carrier concentrations observed are in very good agreement with those expected to arise from the combined effects of spontaneous and piezoelectric polarization. At higher Al concentrations, the data are consistent with partial strain relaxation in the

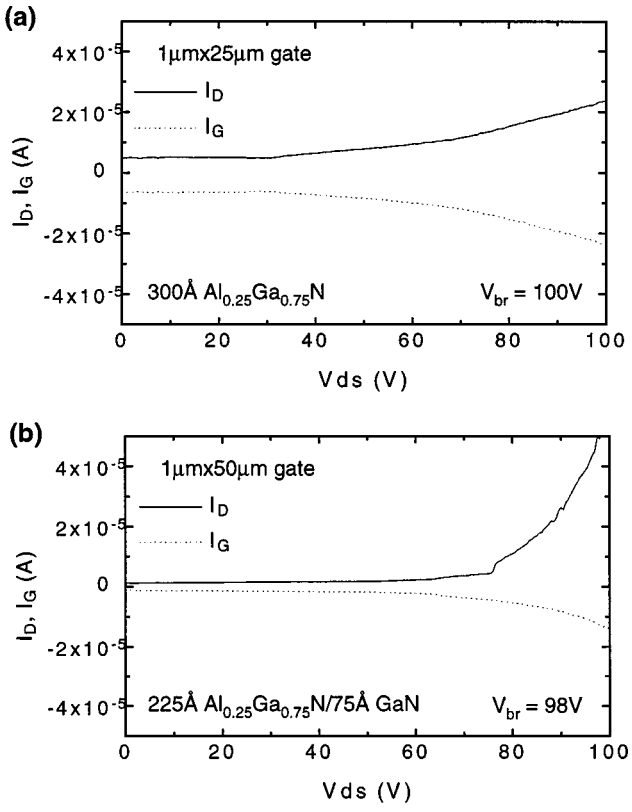

FIG. 9. Off-state gate and drain current as functions of source-drain voltage for (a) conventional-barrier and (b) enhanced-barrier HFET structures, yielding breakdown voltages of 100 and 98 V, respectively.

$Al_xGa_{1-x}N$ barrier layer, which would be accompanied by a reduction in the piezoelectric contribution to polarization charge at the heterojunction interface; an additional possibility is formation of compensating defects in the $Al_xGa_{1-x}N$ layers. Theoretical analysis has indicated that incorporation of In into the barrier and/or channel layers can substantially increase the polarization charge present at the 2DEG heterojunction interface. The use of polarization effects to engineer Schottky barrier structures with substantially increased barrier heights has also been discussed, and current–voltage characteristics of HFETs incorporating either conventional $Al_xGa_{1-x}N$ barriers or polarization-enhanced barriers have been presented. The increase in barrier height in the polarization-enhanced structures leads to a marked suppression in gate leakage current but has a negligible effect on transistor breakdown voltage, as breakdown in these transistor structures was found to be dominated by impact ionization rather that gate tunneling.

ACKNOWLEDGMENTS

The authors are grateful to Dr. J. M. Van Hove of SVT Associates, Inc. and Dr. J. M. Redwing and Dr. K. S. Boutros of Epitronics for providing data concerning sheet carrier concentrations in $Al_xGa_{1-x}N$/GaN HFETs grown, respectively, by MBE and MOCVD. The authors would like to acknowledge financial support from BMDO (Dr. Kepi Wu). One of the authors (E.T.Y.) would like to acknowledge financial support from the Alfred P. Sloan Foundation.

[1]S. Nakamura and G. Fasol, *The Blue Laser Diode: GaN Based Light Emitters and Lasers* (Springer, Berlin, 1997).
[2]M. A. Khan, Q. Chen, M. S. Shur, B. T. McDermott, J. A. Higgins, J. Burm, W. J. Schaff, and L. F. Eastman, IEEE Electron Device Lett. **17**, 584 (1996).
[3]O. Aktas, Z. F. Fan, A. Botchkarev, S. N. Mohammad, M. Roth, T. Jenkins, L. Kehias, and H. Morkoç, IEEE Electron Device Lett. **18**, 293 (1997).
[4]Y. F. Wu, B. P. Keller, S. Keller, D. Kapolnek, P. Kozodoy, S. P. DenBaars, and U. K. Mishra, Appl. Phys. Lett. **69**, 1438 (1996).
[5]G. J. Sullivan, M. Y. Chen, J. A. Higgins, J. W. Yang, Q. Chen, R. L. Pierson, and B. T. McDermott, IEEE Electron Device Lett. **19**, 198 (1998).
[6]S. C. Binari, J. M. Redwing, G. Kelner, and W. Kruppa, Electron. Lett. **33**, 242 (1997).
[7]J. M. Van Hove, R. Hickman, J. J. Klaassen, P. P. Chow, and P. P. Ruden, Appl. Phys. Lett. **70**, 2282 (1997).
[8]Q. Chen, J. W. Yang, A. Osinsky, S. Gangyopadhyay, B. Lim, M. Z. Anwar, M. A. Khan, D. Kuksenkov, and H. Temkin, Appl. Phys. Lett. **70**, 2277 (1997).
[9]R. D. Underwood, S. Keller, U. K. Mishra, D. Kapolnek, B. P. Keller, and S. P. DenBaars, J. Vac. Sci. Technol. B **16**, 822 (1998).
[10]T. Kozawa, M. Suzuki, Y. Taga, Y. Gotoh, and J. Ishikawa, J. Vac. Sci. Technol. B **16**, 833 (1998).
[11]A. Bykhovski, B. Gelmont, and M. S. Shur, J. Appl. Phys. **74**, 6734 (1993).
[12]P. M. Asbeck, E. T. Yu, S. S. Lau, G. J. Sullivan, J. Van Hove, and J. M. Redwing, Electron. Lett. **33**, 1230 (1997).
[13]E. T. Yu, G. J. Sullivan, P. M. Asbeck, C. D. Wang, D. Qiao, and S. S. Lau, Appl. Phys. Lett. **71**, 2794 (1997).
[14]R. Gaska, J. W. Yang, A. D. Bykhovski, M. S. Shur, V. V. Kaminski, and S. M. Soloviov, Appl. Phys. Lett. **72**, 64 (1998).
[15]F. Bernardini, V. Fiorentini, and D. Vanderbilt, Phys. Rev. B **56**, R10024 (1997).
[16]E. S. Hellman, MRS Int. J. Nitride Semicond. Res. **3**, 11 (1998).
[17]R. M. Martin, Phys. Rev. B **5**, 1607 (1972).
[18]S. Strite, M. E. Lin, and H. Morkoç, Thin Solid Films **231**, 197 (1993).
[19]G. D. O'Clock, Jr. and M. T. Duffy, Appl. Phys. Lett. **23**, 55 (1973).
[20]M. A. Littlejohn, J. R. Hauser, and T. H. Glisson, Appl. Phys. Lett. **26**, 625 (1975).
[21]A. D. Bykhovski, V. V. Kaminski, M. S. Shur, Q. C. Chen, and M. A. Khan, Appl. Phys. Lett. **68**, 818 (1996).
[22]A. D. Bykhovski, B. L. Gelmont, and M. S. Shur, J. Appl. Phys. **81**, 6332 (1997).
[23]J. G. Gualtieri, J. A. Kosinski, and A. Ballato, IEEE Trans. Ultrason. Ferroelectr. Freq. Control **41**, 53 (1994).
[24]V. A. Savastenko and A. U. Sheleg, Phys. Status Solidi A **48**, K135 (1978).
[25]Y. Takagi, M. Ahart, T. Azuhata, T. Sota, K. Suzuki, and S. Nakamura, Physica B **219&220**, 547 (1996).
[26]A. Polian, M. Grimsditch, and I. Grzegory, J. Appl. Phys. **79**, 3343 (1996).
[27]R. B. Schwarz, K. Khachaturyan, and E. R. Weber, Appl. Phys. Lett. **70**, 1122 (1997).
[28]C. Deger, E. Born, H. Angerer, O. Ambacher, M. Stutzmann, J. Hornsteiner, E. Riha, and G. Fischerauer, Appl. Phys. Lett. **72**, 2400 (1998).
[29]K. Tsubouchi and N. Mikoshiba, IEEE Trans. Sonics Ultrason. **SU-32**, 634 (1985).
[30]L. E. McNeil, M. Grimsditch, and R. H. French, J. Am. Ceram. Soc. **76**, 1132 (1993).
[31]K. Kim, W. R. L. Lambrecht, and B. Segall, Phys. Rev. B **53**, 16310 (1996).
[32]A. F. Wright, J. Appl. Phys. **82**, 2833 (1997).
[33]T. Takeuchi, S. Sota, M. Katsuragawa, M. Komori, H. Takeuchi, H. Amano, and I. Akasaki, Jpn. J. Appl. Phys., Part 2 **36**, L382 (1997).
[34]M. B. Nardelli, K. Rapcewicz, and J. Bernholc, Appl. Phys. Lett. **71**, 3135 (1997).
[35]T. Takeuchi, C. Wetzel, S. Yamaguchi, H. Sakai, H. Amano, I. Akasaki,

Y. Kaneko, S. Nakagawa, Y. Yamaoka, and N. Yamada, Appl. Phys. Lett. **73**, 1691 (1998).
[36]S. F. Chichibu, A. C. Abare, M. S. Minsky, S. Keller, S. B. Fleischer, J. E. Bowers, E. Hu, U. K. Mishra, L. A. Coldren, S. P. DenBaars, and T. Sota, Appl. Phys. Lett. **73**, 2006 (1998).
[37]H. S. Kim, J. Y. Lin, H. X. Jiang, W. W. Chow, A. Botchkarev, and H. Morkoç, Appl. Phys. Lett. **73**, 3426 (1998).
[38]C. C. Shi, P. M. Asbeck, and E. T. Yu, Appl. Phys. Lett. **74**, 573 (1999).
[39]E. T. Yu, X. Z. Dang, L. S. Yu, D. Qiao, P. M. Asbeck, S. S. Lau, G. J. Sullivan, K. S. Boutros, and J. M. Redwing, Appl. Phys. Lett. **73**, 1880 (1998).
[40]R. D. Underwood, P. Kozodoy, S. Keller, S. P. DenBaars, and U. K. Mishra, Appl. Phys. Lett. **73**, 405 (1998).
[41]A. D. Bykhovski, R. Gaska, and M. S. Shur, Appl. Phys. Lett. **73**, 3577 (1998).
[42]L. S. Yu, D. J. Qiao, Q. J. Xing, S. S. Lau, K. S. Boutros, and J. M. Redwing, Appl. Phys. Lett. **73**, 238 (1998).
[43]X. Z. Dang, R. J. Welty, D. Qiao, P. M. Asbeck, S. S. Lau, E. T. Yu, K. S. Boutros, and J. M. Redwing, Electron. Lett. **35**, 602 (1999).